



**HAL**  
open science

## Broken seniority symmetry in the semimagic proton mid-shell nucleus $95\text{Rh}$

B Das, B Cederwall, C Qi, M Górska, P.H Regan, Ö Aktas, H.M Albers, A Banerjee, M.M.R Chishti, J Gerl, et al.

► **To cite this version:**

B Das, B Cederwall, C Qi, M Górska, P.H Regan, et al.. Broken seniority symmetry in the semimagic proton mid-shell nucleus  $95\text{Rh}$ . *Physical Review Research*, 2024, 6 (2), pp.L022038. 10.1103/PhysRevResearch.6.L022038 . hal-04574352

**HAL Id: hal-04574352**

**<https://hal.science/hal-04574352v1>**

Submitted on 22 Nov 2024



**HAL** is a multi-disciplinary open access archive for the deposit and dissemination of scientific research documents, whether they are published or not. The documents may come from teaching and research institutions in France or abroad, or from public or private research centers.

L'archive ouverte pluridisciplinaire **HAL**, est destinée au dépôt et à la diffusion de documents scientifiques de niveau recherche, publiés ou non, émanant des établissements d'enseignement et de recherche français ou étrangers, des laboratoires publics ou privés.



Distributed under a Creative Commons Attribution 4.0 International License

Broken seniority symmetry in the semimagic proton mid-shell nucleus  $^{95}\text{Rh}$ 

B. Das <sup>1,2,\*</sup> B. Cederwall <sup>1,†</sup> C. Qi,<sup>1</sup> M. Górska,<sup>2</sup> P. H. Regan,<sup>3,4</sup> Ö. Aktas,<sup>1</sup> H. M. Albers,<sup>2</sup> A. Banerjee,<sup>2,‡</sup> M. M. R. Chishti,<sup>3</sup> J. Gerl,<sup>2</sup> N. Hubbard,<sup>2,5,6</sup> S. Jazrawi,<sup>3,4</sup> J. Jolie,<sup>7</sup> A. K. Mistry,<sup>2,5</sup> F. Nowacki,<sup>8</sup> M. Polettini,<sup>9,10</sup> A. Yaneva,<sup>2,7</sup> U. Ahmed,<sup>5,6</sup> S. Alhomaidhi,<sup>2,5,6,11</sup> A. Algora,<sup>12,13</sup> C. Appleton,<sup>14</sup> T. Arici,<sup>2</sup> S. Bagchi,<sup>15</sup> G. Benzoni,<sup>10</sup> J. Benito,<sup>16</sup> A. Blazhev,<sup>7</sup> P. Boutachkov,<sup>2</sup> A. Bracco,<sup>9,10</sup> A. M. Bruce,<sup>17</sup> M. Brunet,<sup>3</sup> R. Canavan,<sup>3,4</sup> T. Davinson,<sup>14</sup> T. Dickel,<sup>2,18</sup> A. Esmaylzadeh,<sup>7</sup> L. M. Fraile,<sup>16</sup> E. Haettner,<sup>2</sup> O. Hall,<sup>14</sup> G. Häfner,<sup>19,7</sup> H. Heggen,<sup>2</sup> Ch. Hornung,<sup>2</sup> J. P. Hucca,<sup>5</sup> P. R. John,<sup>5</sup> D. Kahl,<sup>14</sup> V. Karayonchev,<sup>7</sup> R. Kern,<sup>5</sup> R. Knöbel,<sup>2</sup> A. Korgul,<sup>20</sup> G. Kosir,<sup>21,22</sup> I. Kojouharov,<sup>2</sup> D. Kostyleva,<sup>2</sup> N. Kuzminchuk,<sup>2</sup> N. Kurz,<sup>2</sup> R. Liotta,<sup>1</sup> R. Lozeva,<sup>19</sup> M. Mikolajczuk,<sup>20,2</sup> I. Mukha,<sup>2</sup> P. Napiralla,<sup>5</sup> R. Page,<sup>23</sup> C. M. Petrache,<sup>19</sup> N. Pietralla,<sup>5</sup> S. Pietri,<sup>2</sup> W. R. Plaß,<sup>2,18</sup> Zs. Podolyák,<sup>3</sup> J.-M. Régis,<sup>7</sup> M. Rudigier,<sup>5</sup> H. Rösch,<sup>5</sup> P. Ruotsalainen,<sup>24</sup> E. Sahin,<sup>2,5,6</sup> V. Sánchez-Tembleque,<sup>16</sup> H. Schaffner,<sup>2</sup> C. Scheidenberger,<sup>2</sup> F. Schirru,<sup>2</sup> L. Sexton,<sup>14</sup> B. S. Nara Singh,<sup>25</sup> A. Sharma,<sup>26</sup> R. Shearman,<sup>4</sup> M. Si,<sup>19</sup> Y. K. Tanaka,<sup>27</sup> J. Vasiljević,<sup>1</sup> J. Vesić,<sup>21</sup> J. Vilhena,<sup>28</sup> H. Weick,<sup>2</sup> H. J. Wollersheim,<sup>2</sup> V. Werner,<sup>5,6</sup> J. Wiederhold,<sup>5</sup> W. Witt,<sup>5</sup> P. J. Woods,<sup>14</sup> G. Zimba,<sup>24</sup> and J. Zhao<sup>2</sup>

<sup>1</sup>KTH Royal Institute of Technology, 10691 Stockholm, Sweden

<sup>2</sup>GSI Helmholtzzentrum für Schwerionenforschung GmbH - Darmstadt, 64291 Germany

<sup>3</sup>Department of Physics, University of Surrey - Guildford, GU2 7XH, UK

<sup>4</sup>National Physical Laboratory - Teddington, Middlesex, TW11 0LW, UK

<sup>5</sup>Institut für Kernphysik, Technische Universität Darmstadt - Darmstadt, 64289 Germany

<sup>6</sup>Helmholtz Forschungsakademie Hessen für FAIR (HFHF), GSI Helmholtzzentrum für Schwerionenforschung, Campus Darmstadt, 64289 Darmstadt, Germany

<sup>7</sup>Institut für Kernphysik der Universität zu Köln - Zùlpicher Strasse 77, D-50937 Köln, Germany

<sup>8</sup>Université de Strasbourg, CNRS, IPHC UMR 7178, F-67000 Strasbourg, France

<sup>9</sup>Dipartimento di Fisica, Università degli Studi di Milano - Milano, 20133 Italy

<sup>10</sup>INFN, Sezione di Milano - Milano, 20133 Italy

<sup>11</sup>King Abdulaziz City for Science and Technology (KACST), Riyadh 11442, Saudi Arabia

<sup>12</sup>Instituto de Física Corpuscular, CSIC-Universidad de Valencia - E-46100 Valencia, Spain

<sup>13</sup>Institute for Nuclear Research (ATOMKI), Bem ter 18/c, H-4026 Debrecen, Hungary

<sup>14</sup>University of Edinburgh, School of Physics and Astronomy - Edinburgh EH9 3FD, UK

<sup>15</sup>Indian Institute of Technology, Dhanbad-826004, Jharkhand, India

<sup>16</sup>Grupo de Física Nuclear and IPARCOS, Universidad Complutense de Madrid, CEI Moncloa - E-28040 Madrid, Spain

<sup>17</sup>School of Computing Engineering and Mathematics, University of Brighton - Brighton, BN2 4AT UK

<sup>18</sup>Justus Liebig University, 35390 Giessen, Germany

<sup>19</sup>Université Paris-Saclay, IJCLab, CNRS/IN2P3, F-91405 Orsay, France

<sup>20</sup>Faculty of Physics, University of Warsaw, PL 02-093, Warsaw, Poland

<sup>21</sup>Jozef Stefan Institute - Jamova cesta 39, 1000 Ljubljana, Slovenia

<sup>22</sup>Faculty of Mathematics and Physics, University of Ljubljana, 1000 Ljubljana, Slovenia

<sup>23</sup>Department of Physics, Oliver Lodge Laboratory, University of Liverpool Liverpool L69 7ZE, UK

<sup>24</sup>University of Jyväskylä - Seminaarinkatu 15, 40014 Jyväskylän yliopisto, Finland

<sup>25</sup>SUPA, School of Computing, Engineering and Physical Sciences, University of the West of Scotland - Paisley, PA1 2BE UK

<sup>26</sup>Department of Physics, Indian Institute of Technology Ropar, Rupnagar-140 001, Punjab, India

<sup>27</sup>High-Energy Nuclear Physics Laboratory, RIKEN, 351-0198 Saitama, Japan

<sup>28</sup>Laboratoire de Physique de la Matière Condensée et Nanostructures, Université Lyon I, CNRS, UMR 5586, Domaine scientifique de la Doua - F-69622 Villeurbanne Cedex, France



(Received 12 October 2022; revised 31 January 2024; accepted 25 April 2024; published 10 May 2024)

Lifetime measurements of low-lying excited states in the semimagic ( $N = 50$ ) nucleus  $^{95}\text{Rh}$  have been performed by means of the fast-timing technique. The experiment was carried out using  $\gamma$ -ray detector arrays consisting of  $\text{LaBr}_3(\text{Ce})$  scintillators and germanium detectors integrated into the DESPEC experimental setup commissioned for the Facility for Antiproton and Ion Research (FAIR) Phase-0, Darmstadt, Germany. The excited

\*Corresponding author: b.das@gsi.de

†Corresponding author: bc@kth.se

‡Present address: Saha Institute of Nuclear Physics, Kolkata-700064, India

states in  $^{95}\text{Rh}$  were populated primarily via the  $\beta$  decays of  $^{95}\text{Pd}$  nuclei, produced in the projectile fragmentation of a 850 MeV/nucleon  $^{124}\text{Xe}$  beam impinging on a  $4\text{ g/cm}^2$   $^9\text{Be}$  target. The deduced electromagnetic E2 transition strengths for the  $\gamma$ -ray cascade within the multiplet structure depopulating from the isomeric  $I^\pi = 21/2^+$  state are found to exhibit strong deviations from predictions of standard shell model calculations which feature approximately conserved seniority symmetry. In particular, the observation of a strongly suppressed E2 strength for the  $13/2^+ \rightarrow 9/2^+$  ground state transition cannot be explained by calculations employing standard interactions. This remarkable result may require revision of the nucleon-nucleon interactions employed in state-of-the-art theoretical model calculations, and might also point to the need for including three-body forces in the Hamiltonian.

DOI: [10.1103/PhysRevResearch.6.L022038](https://doi.org/10.1103/PhysRevResearch.6.L022038)

**Introduction.** One of the most intriguing aspects of nuclear phenomenology is the emergence of regular and simple structural patterns from the complex nuclear many-body correlations. In particular, the vast majority of semimagic nuclei (those with either the number of neutrons,  $N$ , or the number of protons,  $Z$ , corresponding to a filled quantum shell) are characterized by the pairwise coupling of the valence nucleons in the unfilled shell [1]. The seniority quantum number,  $\nu$ , is defined as the number of neutrons or protons that are not coupled in pairs to angular momentum  $J = 0$  [2]. Characteristic, regular energy spectra and special patterns of the electric quadrupole transition strengths between the member states of the corresponding seniority multiplets arise as a combined effect of the strong spin-orbit coupling and residual pairing correlations in the nuclear mean field.

Even though seniority is an approximate symmetry it hence has a profound impact on the description of the spectroscopic and electromagnetic transition properties of nuclei near closed quantum shells. It is a strictly conserved quantum number for systems with identical particles in a single- $j$  angular momentum subshell with  $j \leq 7/2$  in the presence of an attractive two-body pairing force. Even for systems with higher  $j$  values, like for particles in the  $g_{9/2}$ ,  $j = 9/2$  subshell, the seniority-violating interaction matrix elements are expected to be negligible in most empirical shell model interactions. The  $j = 9/2$  case has recently received particular interest with respect to the special partial conservation of seniority in systems with four proton particles/holes [3–10].

A striking consequence of seniority symmetry is that the squares of the  $\Delta\nu = 0$  matrix elements of even-tensor one- and two-particle operators, such as the electromagnetic quadrupole (E2) operator, are symmetric with respect to the middle of the angular momentum subshell, i.e., when the number of particles occupying levels in the angular momentum subshell is  $n_j = (2j + 1)/2$ . This can be considered to be a result of the combination of particle-hole conjugation and seniority conservation, intertwined through a Berry phase [11]. The corresponding transition probabilities between such states therefore vanish when the Fermi level is situated in the middle of the subshell, as is the case for  $^{95}\text{Rh}$ . Converseley, the seniority changing  $\Delta\nu = 2$  matrix elements of the same operators, which mirror the behavior of the seniority conserving matrix elements as a function of shell filling, are maximal at midshell.

The few observed exceptions from the general rule of energy level spectra and E2 transition rates following the

predictions of shell model calculations with a seniority conserving nuclear interaction are particularly interesting since they may reveal otherwise hidden details of the nuclear force. Such cases include the semimagic ( $N = 50$ ) nuclei  $^{94}\text{Ru}$  and  $^{96}\text{Pd}$ , for which there are large discrepancies between the observed  $4^+ \rightarrow 2^+$  electromagnetic E2 transition strengths and theoretical predictions in different directions [7,12–16]. For these nuclei, the valence protons occupy the upper half of the  $N/Z = 28 - 50$  major shell which is characterized by the relative isolation of the  $g_{9/2}$  subshell. Mach *et al.* reported a lower limit,  $B(E2:4^+ \rightarrow 2^+) \geq 46 e^2 fm^4$  for  $^{94}\text{Ru}$  and a value  $B(E2:4^+ \rightarrow 2^+) = 3.8(4) e^2 fm^4$  for  $^{96}\text{Pd}$ , corresponding to strongly enhanced and retarded  $4^+ \rightarrow 2^+$  E2 transition strengths, respectively, compared with seniority-conserving shell model predictions [7]. They suggested that the observed anomalous E2 strengths in these  $N = 50$  isotones and the inferred seniority symmetry breaking is due to residual neutron-proton interactions in combination with neutron particle-hole (ph) excitations across the  $N = 50$  shell gap. Das *et al.* recently reported a value  $B(E2:4^+ \rightarrow 2^+) = 103(24) e^2 fm^4$  for the same transition in  $^{94}\text{Ru}$  [12] and proposed, alternatively, the observed seniority symmetry breaking effect in  $^{94}\text{Ru}$  to be a result of a subtle interference between the wave functions of the initial and final states induced by cross-orbital interactions within the major valence shell. Subsequently, Pérez-Vidal *et al.* reported a value  $B(E2:4^+ \rightarrow 2^+) = 38(3) e^2 fm^4$  for  $^{94}\text{Ru}$ , differing significantly from the previously reported results [7,12], and arrived at a different conclusion, namely, that seniority is largely conserved in the first  $\pi g_{9/2}$  orbital [13]. This situation requires further investigation, both from an experimental and theoretical stand point.

The nucleus  $^{95}_{45}\text{Rh}_{50}$  is located exactly at the  $\pi g_{9/2}$  midshell and should therefore exhibit approximate particle-hole symmetry, i.e., it can be described both as five valence protons and five proton holes in the  $g_{9/2}$  orbital. A puzzling enhancement of the  $B(E2)$  strength in this nucleus has previously been reported [7,14–16] for the  $21/2^+ \rightarrow 17/2^+$  transition instead of the near-vanishing E2 transition rate expected from approximate seniority conservation for a  $\Delta\nu = 0$  transition.

In this Letter we present lifetime measurements on the low-lying yrast states of  $^{95}\text{Rh}$  using the direct, fast-timing method. The extracted E2 transition strengths are compared with the results from large-scale shell-model and single- $j$  shell calculations. A strong violation of the seniority coupling scheme is observed, which cannot be reproduced by state-of-the-art

empirical shell model interactions applied in different model spaces.

*Experiment details and data analysis.* Lifetime measurements of low-lying yrast states of  $^{95}\text{Rh}$  were performed using the DEcay SPECTroscopy (DESPEC) [17] setup commissioned for the Facility for Antiproton and Ion Research (FAIR) [18,19] Phase-0. The results presented here were obtained from the same measurement as those previously reported for  $^{94}\text{Ru}$  [12].

$^{124}\text{Xe}$  ions were accelerated to a kinetic energy of 850 MeV/u by the SIS-18 synchrotron at the GSI Helmholtzzentrum für Schwerionenforschung accelerator facility, Darmstadt, Germany, and impinged on a  $^9\text{Be}$  target of  $4\text{ g/cm}^2$  areal density. Nuclear fragments produced in the reactions were identified and transported to the final focal plane of the FRagment Separator (FRS) using the  $B\rho$ - $\Delta E$ - $B\rho$  and ToF- $B\rho$ - $\Delta E$  methods [20,21]. The Advanced Implantation Detector Array (AIDA) [22,23], composed of three double-sided silicon strip detectors (DSSSD), was used to stop the product nuclei and to measure their subsequent charged-particle decays. The White Rabbit (WR) [24] clock was used to save the implant timing. WR is a common clock to all DESPEC subsystems and used to synchronize these subsystems with 1 ns precision. As a result, the timing information of each implanted  $^{95}\text{Pd}$  ion was saved as a function of its position,  $(x, y)$ , where  $x$  and  $y$  are the horizontal and vertical strip numbers of the DSSSD, respectively. After implantation of the  $^{95}\text{Pd}$  ions, population of the  $21/2^+$  isomer leads to  $\beta$  decay into the analog spin-parity state of the  $^{95}\text{Rh}$  nucleus [25], which then de-excites toward the  $9/2^+$  ground state via a cascade of stretched  $\gamma$ -ray transitions. To identify such  $\beta$ -delayed  $\gamma$  rays,  $\beta$  decays correlated with implants of the  $^{95}\text{Pd}$  ions were searched for within the DSSSD pixels. The time correlation was obtained using the WR clock with a  $\sim 3 \times T_{1/2}$  ( $T_{1/2} = 14(1)\text{s}$  [25]) time window, within which the  $\beta$ -decay pixel position was validated if an ion had been implanted in the same pixel or in any of its immediate neighbors, taking into account that the highly penetrating  $\beta$  rays may scatter to the neighboring pixels from the implantation point depositing partial or full energy.

The  $\beta$ -delayed  $\gamma$  rays were registered using an array of six triple-cluster germanium detectors [19], and an array of 36  $\text{LaBr}_3(\text{Ce})$  detectors. The latter, with its much faster time response, is known as the FAst TIMing Array (FATIMA) [26–28]. The WR timestamps were used to find  $\beta$ - $\gamma$  correlations, where the slow time response of the decay amplifier in AIDA (read-out time  $\sim 2\mu\text{s}$ ) opens up a wide time correlation window. The  $\beta$ - $\gamma$  events lie within the peak of the time distribution,  $\delta T$ , of  $\gamma$  rays detected in FATIMA relative to the  $\beta$ -decay time registered in AIDA, see Fig. 1(b). Clean mutual coincidences could be obtained between the 381 keV( $21/2^+ \rightarrow 17/2_1^+$ ), 716 keV( $17/2_1^+ \rightarrow 13/2^+$ ), and 1351 keV( $13/2^+ \rightarrow 9/2^+$ )  $\gamma$  lines below the seniority isomer in  $^{95}\text{Rh}$  [25]. The presence of transitions decaying to the  $13/2^+$  state could be observed in the 1351 keV gated spectra of  $\beta$ - $\gamma$ - $\gamma$  events in Fig. 1(a). The reported energies were measured using the germanium detectors and agree with the previous assignments [15,16,29].

The FATIMA  $\text{LaBr}_3(\text{Ce})$  detectors were used to measure direct  $\gamma$ - $\gamma$  time differences, with a resolution of 25 ps least significant bit [17]. Mean level lifetimes ( $\tau$ ) for the yrast

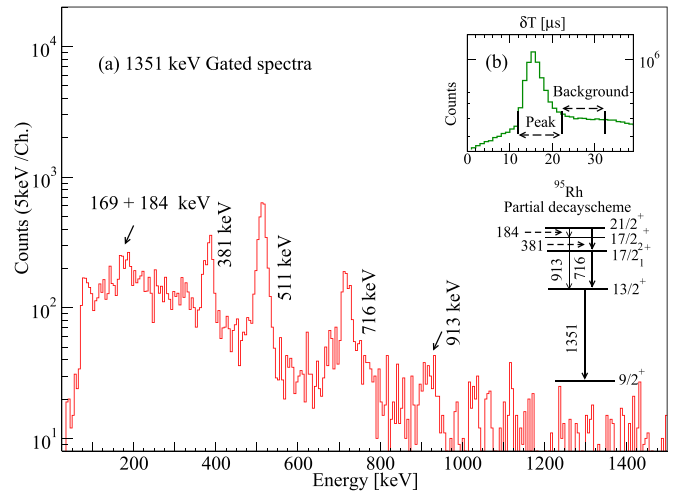


FIG. 1. (a) The  $\gamma$  energies of  $\beta$ - $\gamma$ - $\gamma$  events in coincidence with 1351 keV transition. The decay of  $I^\pi = 21/2^+$  is depicted at the inset, while the 169 keV transition is coming from the decay of the  $I^\pi = 17/2^-$  isomer. (b) The WR time difference between AIDA and FATIMA for the  $\beta$ -decay events from  $^{95}\text{Pd}$ .

states of  $^{95}\text{Rh}$  were deduced using the generalized centroid difference (GCD) method [30,31]. The centroid difference for a coincident  $\gamma$ -ray pair,  $\Delta C$ , is directly related to  $\tau$ , following the relation

$$\Delta C(\Delta E_\gamma) = \Delta PRD(\Delta E_\gamma) + 2\tau, \quad (1)$$

with the symmetry conditions [31]

$$\begin{aligned} \Delta C(\Delta E_\gamma) &= -\Delta C(-\Delta E_\gamma), \\ PRD(\Delta E_\gamma) &= -PRD(-\Delta E_\gamma), \end{aligned} \quad (2)$$

where  $\Delta E_\gamma$  is the energy difference between the feeding and the decaying  $\gamma$  rays of the level, and PRD is the prompt response difference [30]. The calibration measurement of the PRD function for the present setup has been described in Ref. [12].

The delayed and antidelated time distributions obtained for the  $13/2^+$  and  $17/2_1^+$  states are shown in Figs. 2(a) and 2(d), respectively, from which the generalized time centroids [32] were obtained. The background contribution to the time distribution was subtracted according to the method described in Ref. [33]. The time spectra due to background coincidences are shown in Figs. 2(b) and 2(c) and Figs. 2(e) and 2(f) for the  $13/2^+$  and  $17/2_1^+$  states, respectively. The PRD values of  $-321(\pm 6 \pm 14 \pm 16)$  ps and  $-290(\pm 6 \pm 14 \pm 15)$  ps were obtained from the fit shown in Fig. 2(b) of Ref. [12], for the  $13/2^+$  and  $17/2_1^+$  states, respectively. The PRD errors in bracket include the time uncertainty introduced by the large energy width of  $\text{LaBr}_3$  detectors, along with the fit residual errors for start and stop energies, respectively. One may note that this is the only source of systematic errors built into the GCD method [30]. The cancellation of systematic errors from different sources therefore makes it advantageous over other fast-timing methods. The obtained lifetime values are  $\tau(13/2_1^+) = 36(15)$  ps and  $\tau(17/2_1^+) = 8(18)$  ps, the latter corresponding to a limit  $\tau(17/2_1^+) \leq 26$  ps with  $1\sigma$  uncertainty. The uncertainties include uncorrelated errors added



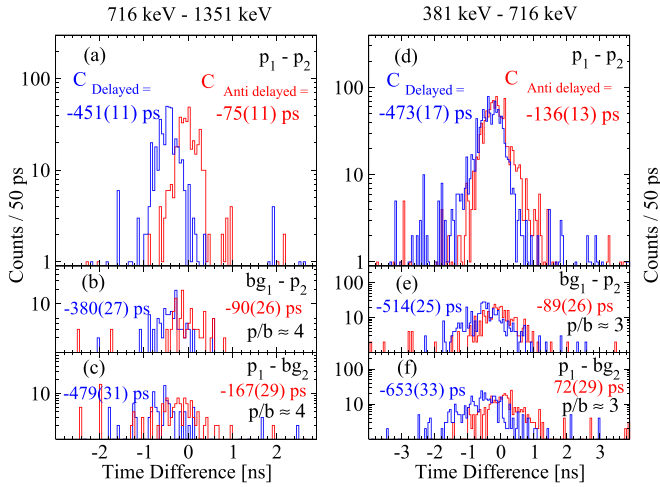


FIG. 2. Delayed and antidelayed time distributions for the (a) 381 keV ( $p_1$ )–716 keV ( $p_2$ ) transitions, where (b) and (c) depict peak-to-background ( $p$ - $bg$ ) coincidences. Delayed and antidelayed time distributions for the (d) 716 keV–1351 keV transitions, where (e) and (f) depict peak-to-background coincidences.

in quadrature [34]. The use of the GCD method with the present experimental setup was also validated by remeasuring the mean lives of the  $4_1^+$  and  $2_1^+$  states in  $^{94}\text{Ru}$  and  $^{96}\text{Pd}$  from the same experiment. For  $^{94}\text{Ru}$ , the lifetimes of the  $4_1^+$  and  $2_1^+$  states were observed to be  $\tau = 32(11)$  ps and  $\tau \leq 14$  ps, respectively [12], and consistent with the respective  $\tau \leq 72$  ps and  $\tau \leq 14$  ps limits previously established by Mach *et al.* [7]. For  $^{96}\text{Pd}$ , Yaneva *et al.*, [35] have measured the value  $\tau(4_1^+) = 1.44(7)$  ns and the limit  $\tau(2_1^+) \leq 20$  ps, which also confirms the previous measurements [7]. It is to be noted that, despite the similar  $\Delta E_\gamma$  values for the first excited states in these nuclei, the delayed nature of the  $13/2_1^+ \rightarrow 9/2^+$  transition could be clearly established for  $^{95}\text{Rh}$ . The lifetime of the  $17/2_2^+$  state of  $^{95}\text{Rh}$  [15] could not be measured in the present experiment due to insufficient statistics. The experimental results are summarized in Table I.

**Discussion.** To understand the observed E2 transition properties of the low-lying yrast structure in  $^{95}\text{Rh}$ , we have carried out configuration interaction model calculations including extensive large-scale shell model (LSSM) calculations in a variety of model spaces, and compared the results with those from a pure single- $j$  shell calculation. In Fig. 3 the experimental low-lying yrast spectrum and the associated E2 transition strengths

TABLE I. Experimental lifetimes and  $B(E2)$  strengths in  $^{95}\text{Rh}$ . The lifetime value for the  $21/2^+$  state is taken from Ref. [16]. The lifetime limit for the  $17/2_1^+$  state was determined with a 1 $\sigma$  confidence level. See text for details.

$I_i^\pi \rightarrow I_f^\pi$	$\tau$ [ps]	$B_{\text{exp.}}(E2)$ [ $e^2 \text{fm}^4$ ]
$21/2^+ \rightarrow 17/2_1^+$	$3.0(4) \times 10^3$	$29.0(4.0)$ [7]
$21/2^+ \rightarrow 17/2_2^+$	$3.0(4) \times 10^3$	$136(20)$ [7]
$17/2_1^+ \rightarrow 13/2_1^+$	$\leq 26$	$\geq 167$
$17/2_2^+ \rightarrow 13/2_1^+$		
$13/2_1^+ \rightarrow 9/2^+$	$36(15)$	$5.0^{+3.6}_{-1.6}$

between the members of the  $\pi g_{9/2}$  seniority multiplet are compared with theoretical calculations using the single  $\pi g_{9/2}$  (labeled “g”) model space with the same seniority-conserving empirical interaction as used in Ref. [36], the  $\pi f_{5/2} p_{1/2,3/2} g_{9/2}$  (labeled “fpg”) model space with the jun45 interaction [37], and the  $\pi \nu g_{9/2,7/2} d_{5/2,3/2} s_{1/2}$  model space (labeled “gds”), employing the SDG CD-Bonn based G-matrix renormalized SDGN interaction [7,38], limiting the model space to allow a maximum of  $t = 6$  particles that can be excited across the  $N = Z = 50$  major shell. Effective charges of  $e_p(e_n) = 1.5e(0.5e)$  were used for the calculations in the “g” and “fpg” model spaces and  $e_p(e_n) = 1.11e(0.84e)$  [39] in the “gds” model space. Numerical results are listed in Table II. The  $\nu = 3$ -dominated,  $17/2^+$  state is predicted to be lower in excitation energy than the  $\nu = 5$ -dominated state in the “g” and “gds” model spaces, whereas an inversion between the two states is seen in the “fpg” space calculation. However, predicted energy spectra and electromagnetic transition strengths for the different model calculations are in general quite similar, in excellent agreement with approximate seniority symmetry. On the other hand, it may be immediately recognized that the calculated electromagnetic transition strengths are in stark contrast with the experimental observations. In particular, none of the calculations are even close to reproducing the experimentally observed E2 transition rate for the  $13/2_1^+ \rightarrow 9/2^+$  ground-state transition.

The five protons in the  $0g_{9/2}$  subshell can couple to three  $I^\pi = 9/2^+$ ;  $\nu = 1, 3, 5$ , states, two  $13/2^+$ ;  $\nu = 3, 5$ , and two  $17/2^+$ ;  $\nu = 3, 5$  states. The  $I^\pi = 9/2^+$  ground state and the first  $I^\pi = 13/2^+$  state (which is dominated by  $\nu = 3$ ) are predicted to be well separated in energy in calculations employing a variety of standard effective interactions in different model spaces while the two  $I^\pi = 17/2^+$  states can be close to each other [9]. A special property of midshell nuclei like  $^{95}\text{Rh}$  is that the two-body interaction, operating within a single- $j$  shell, can only mix configurations with seniority differing by  $\Delta\nu = 4$ . This means that the two  $13/2^+$  and  $17/2^+$  states with  $\nu = 3$  and 5 never mix in such calculations and the seniority symmetry is strictly conserved. In general, the  $13/2_2^+$  state (dominated by  $\nu = 5$ ) is predicted at much higher excitation energy than the first  $13/2_1^+$  ( $\nu = 3$ ) state, at 3.03 MeV in the g calculation and 2.94 MeV in the fpg model space. The state is calculated to decay primarily to the  $17/2^+$   $\nu = 3$ -dominated state or a  $11/2^+$  state.

In general, the wave function of a state  $|\alpha\rangle$  with angular momentum quantum number  $I$  can be expressed as a superposition of single- $j$  configurations with different seniority and configurations as

$$|I, \alpha\rangle = \sum_{\nu=1,3,5} c_\nu |(0g_{9/2}^5, \nu, I)\rangle + \text{contributions from other shells.} \quad (3)$$

The three  $I^\pi = 9/2^+$  configurations can mix with each other due to the allowed  $\Delta\nu = 4$  mixing between the  $\nu = 1$  and  $\nu = 5$  configurations and interactions with the intermediate  $\nu = 3$  state via mainly the close-lying  $p_{1/2}$  subshell. However, the mixing between the  $\nu = 1$   $I^\pi = 9/2^+$  ground state and the  $\nu = 3$  and  $\nu = 5$   $I^\pi = 9/2^+$  states is predicted to be quite small (1.16% and 2.14%, respectively) due to the dominance

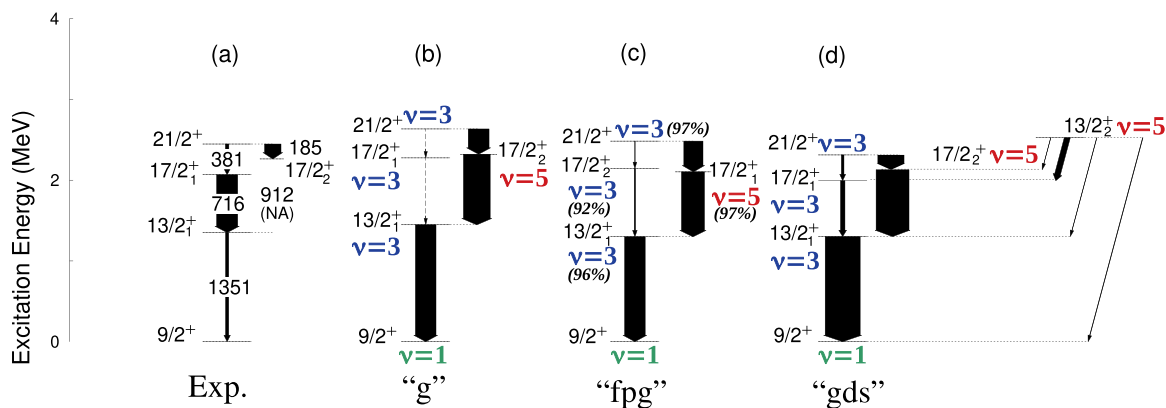


FIG. 3. Experimental and theoretical level energies and electromagnetic transition strengths for the low-lying excited states in  $^{95}\text{Rh}$ . The widths of the arrows are proportional to the experimentally deduced (a) and calculated (b)–(d)  $B(E2)$  values given in Table I and Table II. Dashed arrows correspond to a vanishing transition strength. The theoretically calculated energy levels are labeled by the dominant seniority quantum number in the wave function. For the calculation employing the *jun45* interaction (c), the squared amplitude of the dominant signature component is also given.

of the pairing matrix element which increases the energy of the latter states to around 1.8 MeV and 2.3 MeV, respectively, for the calculation employing the realistic *jun45* interaction [37]. The  $\nu = 3$  and  $\nu = 5$  admixtures in the ground state wave function are consistently zero or of similar magnitude for all the interactions and model spaces employed in this work. The same applies to the predictions for the mixing between the  $13/2_1^+$  and  $13/2_2^+$  states.

A particularly striking feature of the electromagnetic properties of  $^{95}\text{Rh}$  is the observed strong hindrance of the  $13/2_1^+ \rightarrow 9/2^+$  transition, in contradiction to the predictions within the seniority coupling scheme as well as all of our LSSM calculations. The experimentally deduced  $B(E2:13/2_1^+ \rightarrow 9/2^+)$  value of  $5.0_{-1.6}^{+3.6} e^2 fm^4$  is reduced by a factor of more than 30 compared with the lowest theoretical prediction obtained in this work (Table II). This indicates a strong violation of seniority symmetry and that the two  $\nu = 3$  and  $\nu = 5$ ,  $13/2^+$  states, unexpectedly, might be strongly mixed. We have therefore evaluated the influence of various nondiagonal matrix element contributions to Eq. (3) by varying their strengths. No significant mixing has been found in our calculations without invoking an unrealistic adjustment of those matrix elements that would lead to strong perturbations in, e.g., the predicted level energies.

We have also extended our calculations to include neutron cross-shell excitations including  $d_{5/2}$  and  $g_{7/2}$  configurations

as in Refs. [40,41]. However, no significant contributions to the wave functions from neutron core excitations across the  $N = 50$  shell closure were found for the lowest  $I^\pi = 9/2^+$ ,  $13/2^+$ , and  $17/2^+$  states, primarily due to the large energy gap ( $\sim 4$  MeV) between the  $g_{9/2}$  subshell and higher-lying shells. It is also noteworthy that no evidence for significant cross-shell excitations was observed for the neutron analog system,  $^{213}\text{Pb}$ , with five neutrons in the  $1g_{9/2}$  shell [11]. There is very limited experimental information on the E2 transition probabilities in similar systems. We note, however, that the deduced limits on the E2 strengths for the  $2_1^+ \rightarrow 0_g^+$  transitions in the neighboring  $N = 50$  isotones  $^{94}\text{Ru}$  [7,12] and  $^{96}\text{Pd}$  [7], which are expected to be similar to the  $13/2_1^+ \rightarrow 9/2^+$  transition in  $^{95}\text{Rh}$ , are in agreement with the predicted behavior for conserved seniority symmetry.

The observed  $13/2_1^+ \rightarrow 9/2_{gs}^+$  E2 transition strength in  $^{95}\text{Rh}$  appears to be extremely difficult to reproduce using standard effective two-body shell model interactions. Although highly challenging and beyond the current state of the art in computational capabilities, it is possible that the inclusion of three-body forces into the shell-model Hamiltonian [42,43] could elucidate the mechanism behind this unexpected observation. For a more complete picture, experimental data on similar systems are also required.

*Acknowledgments.* The results presented here are based on the experiment S480, which was performed at the target station HFS at the GSI Helmholtzzentrum für Schwerionenforschung, Darmstadt (Germany) in the frame of FAIR Phase-0. The authors would like to thank the staff of the GSI accelerator and the technicians of the FRS for their excellent support. This work was supported by the Swedish Research Council under Grants No. 621-2014-5558 and No. 2019-04880. We acknowledge support by the STFC under Grants No. ST/G000697/1, No. ST/P005314, No. ST/P003982/1, No. ST/P004598/1, and No. ST/V001027/1; by the UK Department for Business, Energy and Industrial Strategy via the National Measurement Office; by the BMBF under Grants No. 05P19RDFN1 and No. 05P21RDFN1; by the Helmholtz Research Academy Hesse for FAIR (HFHF); by the GSI F&E

TABLE II. Theoretical  $B(E2)$  strengths in  $^{95}\text{Rh}$  calculated in different model spaces. The states are labeled by the dominant seniority component in the wave function. See text for details.

$I_i^\pi \rightarrow I_f^\pi$	$B_{gds}(E2)$ [ $e^2 fm^4$ ]	$B_{fpg}(E2)$ [ $e^2 fm^4$ ]	$B_g(E2)$ [ $e^2 fm^4$ ]
$21/2^+ \rightarrow 17/2_{\nu=3}^+$	10.7	2.8	0.00
$21/2^+ \rightarrow 17/2_{\nu=5}^+$	177.1	158.1	172.0
$17/2_{\nu=3}^+ \rightarrow 13/2_{\nu=3}^+$	18.4	10.9	0.0
$17/2_{\nu=5}^+ \rightarrow 13/2_{\nu=3}^+$	232.4	189.5	208.7
$13/2_{\nu=3}^+ \rightarrow 9/2^+$	219.2	169.7	169.3

Grant No. KJOLIE1820; and by BMBF Grant 05P19PKFNA. G.H., M.S., and R.L. acknowledge IN2P3-GSI Agreements, ADI-IDEX, and CSC-UPS Grants. L.M.F. acknowledges the Spanish MICINN via Project No. RTI2018-098868-B-100. A.A. acknowledges partial support by the Ministerio de Cien-

cia e Innovacion Grant No. PID2019-104714GB-C21. J.V. acknowledges support by the Slovenian research agency Grant No. IO-0005. B.S.N.S acknowledges the financial support of the UKRI STFC through Grants No. ST/T001739/1 and No. ST/P005101/1.

- [1] John. P. Schiffer and William. W. True, The effective interaction between nucleons deduced from nuclear spectra, *Rev. Mod. Phys.* **48**, 191 (1976).
- [2] G. Racah, Theory of complex spectra. III, *Phys. Rev.* **63**, 367 (1943).
- [3] A. Escuderos and L. Zamick, Seniority conservation and seniority violation in the  $g_{9/2}$  shell, *Phys. Rev. C* **73**, 044302 (2006).
- [4] P. Van Isacker and S. Heinze, Partial conservation of seniority and nuclear isomerism, *Phys. Rev. Lett.* **100**, 052501 (2008).
- [5] P. Van Isacker, Seniority isomers in nuclei, *J. Phys.: Conf. Ser.* **322**, 012003 (2011).
- [6] C. Qi, Partial conservation of seniority in the  $j=9/2$  shell: Analytic and numerical studies, *Phys. Rev. C* **83**, 014307 (2011).
- [7] H. Mach, A. Korgul, M. Gorska, H. Grawe, I. Matea, M. Stanoiu, L. M. Fraile, Y. E. Penionzkevich, F. D. Santos, D. Verney, S. Lukyanov, B. Cederwall, A. Covello, Z. Dlouhy, B. Fogelberg, G. DeFrance, A. Gargano, G. Georgiev, R. Grzywacz, A. F. Lisetskiy, J. Mrazek, F. Nowacki, W. A. Plociennik, Z. Podolyak, S. Ray, E. Ruchowska, M. G. Saint-Laurent, M. Sawicka, C. Stodel, and O. Tarasov, Ultrafast-timing lifetime measurements in  $^{94}\text{Ru}$  and  $^{96}\text{Pd}$ : Breakdown of the seniority scheme in  $N = 50$  isotones, *Phys. Rev. C* **95**, 014313 (2017).
- [8] C. Qi, Partial conservation of seniority and its unexpected influence on E2 transitions in  $g_{9/2}$  nuclei, *Phys. Lett. B* **773**, 616 (2017).
- [9] Y. Qian and C. Qi, Partial seniority conservation and solvability of single- $j$  systems, *Phys. Rev. C* **98**, 061303(R) (2018).
- [10] A. I. Morales, G. Benzoni, H. Watanabe, G. de Angelis, S. Nishimura, L. Coraggio, A. Gargano, N. Itaco, T. Otsuka, Y. Tsunoda *et al.*, Is seniority a partial dynamic symmetry in the first  $\nu g_{9/2}$  shell? *Phys. Lett. B* **781**, 706 (2018).
- [11] J. J. Valiente-Dobón, A. Gottardo, G. Benzoni, A. Gadea, S. Lunardi, A. Algora, G. de Angelis, D. Bazzacco, J. Benlliure, P. Boutachkov *et al.*, Manifestation of the Berry phase in the atomic nucleus  $^{213}\text{Pb}$ , *Phys. Lett. B* **816**, 136183 (2021).
- [12] B. Das, B. Cederwall, C. Qi, M. Górska, P. H. Regan *et al.*, Nature of seniority symmetry breaking in the semimagic nucleus  $^{94}\text{Ru}$ , *Phys. Rev. C* **105**, L031304 (2022).
- [13] R. M. Pérez-Vidal *et al.*, Evidence of partial seniority conservation in the  $\pi g_{9/2}$  shell for the  $N = 50$  isotones, *Phys. Rev. Lett.* **129**, 112501 (2022).
- [14] A. Amusa and R. D. Lawson, High spin states in  $^{94}\text{Ru}$  and  $^{95}\text{Rh}$ , *Z. Phys. A* **307**, 333 (1982).
- [15] A. Jungclaus, D. Kast, K. P. Lieb, C. Teich, M. Weiszflog, T. Härtlein, C. Ender, F. Köck, D. Schwalm, J. Reif *et al.*, Picosecond lifetime measurement of neutron core-excited states in the  $N = 50$  nucleus  $^{95}\text{Rh}$ , *Nucl. Phys. A* **637**, 346 (1998).
- [16] E. Nolte, G. Korschinek, and U. Heim, Investigation of very neutron deficient Ru and Rh nuclei with the help of  $(40\text{Ca}; \gamma p + \alpha \gamma)$  reactions, *Z. Phys. A* **298**, 191 (1980).
- [17] A. K. Mistry *et al.*, The DESPEC setup for GSI and FAIR, *Nucl. Instrum. Methods Phys. Res. Sect. A* **1033**, 166662 (2022).
- [18] P. Spiller and G. Franchetti, The FAIR accelerator project at GSI, *Nucl. Instrum. Methods Phys. Res. Sect. A* **561**, 305 (2006).
- [19] M. Poletini *et al.*, DESPEC Phase-0 campaign at GSI, *NUOVO CIMENTO* **44C**, 67 (2021).
- [20] H. Geissel, P. Armbruster, K.H. Behr, A. Brünle, K. Burkard, M. Chen, H. Folger, B. Franczak, H. Keller, O. Klepper *et al.*, The GSI projectile fragment separator (FRS): a versatile magnetic system for relativistic heavy ions, *Nucl. Instrum. Methods Phys. Res. B* **70**, 286 (1992).
- [21] A. B. Garnsworthy *et al.*, Isomeric states in neutron-deficient  $A \sim 80$ – $90$  nuclei populated in the fragmentation of  $^{107}\text{Ag}$ , *Phys. Rev. C* **80**, 064303 (2009).
- [22] C. J. Griffin *et al.*,  $\beta$ -decay studies of r-process nuclei using the Advanced Implantation Detector Array (AIDA), *JPS Conf. Proc.* **14**, 020622 (2017).
- [23] O. Hall, T. Davinson, C. J. Griffin, P. J. Woods, C. Appleton, C. G. Bruno, A. Estrade, D. Kahl, L. Sexton, I. Burrows *et al.*, The advanced implantation detector array (AIDA), *Nucl. Instrum. Methods Phys. Res. B* **1050**, 168166 (2023).
- [24] J. Serrano *et al.*, The white rabbit project, *Proceedings of ICALEPCS TUC004* (Kobe, Japan, 2009).
- [25] E. Nolte and H. Hick,  $\beta$  delayed proton emission from a long-lived high-spin isomer in  $^{95}\text{Pd}$ , *Phys. Lett. B* **97**, 55 (1980).
- [26] P. H. Regan, Precision measurement of sub-nanosecond lifetimes of excited nuclear states using fast-timing coincidences with  $\text{LaBr}_3(\text{Ce})$  detectors, *Radiat. Phys. Chem.* **116**, 38 (2015).
- [27] M. Rudigier, Zs. Podolyák, P. H. Regan, A. M. Bruce, S. Lalkovski, R. L. Canavan, E. R. Gamba, O. Roberts, I. Burrows, D. M. Cullen *et al.*, FATIMA—FAst TIMing Array for DESPEC at FAIR, *Nucl. Instrum. Methods Phys. Res. Sect. A* **969**, 163967 (2020).
- [28] S. Jazrawi, A. Yaneva, M. Poletini, B. Das, P. H. Regan, M. Górska, B. Cederwall, J. Jolie, H. M. Albers, M. M. R. Chishti *et al.*, Commissioning the FAst TIMing array (FATIMA) at FAIR Phase-0: half-lives of excited states in the  $N = 50$  isotones  $^{96}\text{Pd}$  and  $^{94}\text{Ru}$ , *Radiat. Phys. Chem.* **200**, 110234 (2022).
- [29] H. A. Roth, S. E. Arnell, D. Foltescu, O. Skeppstedt, J. Blomqvist, A. Nilsson, T. Kuroyanagi, S. Mitarai, and J. Nyberg, Gaps in the yrast level structure of the  $N = 50$  isotones  $^{93}\text{Tc}$ ,  $^{94}\text{Ru}$ , and  $^{95}\text{Rh}$  at high angular momentum, *Phys. Rev. C* **50**, 1330 (1994).
- [30] J.-M. Régis *et al.*, The generalized centroid difference method for picosecond sensitive determination of lifetimes of nuclear excited states using large fast-timing arrays, *Nucl. Instrum. Methods Phys. Res. Sect. A* **726**, 191 (2013).
- [31] J.-M. Régis, H. Mach, G. S. Simpson, J. Jolie, G. Pascovici, N. Saed-Samii, N. Warr, A. Bruce, J. Degenkolb, L. M. Fraile

- et al.*, The generalized centroid difference method for lifetime measurements via  $\gamma - \gamma$  coincidences using large fast-timing array, *EPJ Web Conf.* **93**, 01013 (2015).
- [32] J.-M. Régis, G. Pascovici, J. Jolie, and M. Rudigier, The mirror symmetric centroid difference method for picosecond lifetime measurements via  $\gamma - \gamma$  coincidences using very fast LaBr<sub>3</sub> (Ce) scintillator detectors, *Nucl. Instrum. Methods Phys. Res. Sect. A* **622**, 83 (2010).
- [33] J.-M. Régis, J. Jolie, N. Saed-Samii, N. Warr, M. Pfeiffer, A. Blanc, M. Jentschel, U. Koster, P. Mutti, T. Soldner, G. S. Simpson, F. Drouet, A. Vancraeynest, G. deFrance, E. Clement, O. Stezowski, C. A. Ur, W. Urban, P. H. Regan, Z. Podolyak, C. Larijani, C. Townsley, R. Carroll, E. Wilson, L. M. Fraile, H. Mach, V. Pazyi, B. Olaizola, V. Vedia, A. M. Bruce, O. J. Roberts, J. F. Smith, M. Scheck, T. Kroll, A. L. Hartig, A. Ignatov, S. Ilieva, S. Lalkovski, W. Korten, N. Marginean, T. Otsuka, N. Shimizu, T. Togashi, and Y. Tsunoda, Abrupt shape transition at neutron number  $N=60$ :  $B(E2)$  values in <sup>94,96,98</sup>Sr from fast  $\gamma - \gamma$  timing, *Phys. Rev. C* **95**, 054319 (2017).
- [34] J. Erler, On the combination procedure of correlated errors, *Eur. Phys. J. C* **75**, 453 (2015).
- [35] A. Yaneva *et al.*, Fast-timing measurement in <sup>96</sup>Pd : Improved accuracy for the lifetime of the  $4_1^+$  state, *Acta Phys. Pol. B Proc. Suppl.* **16**, 4-A30 (2023).
- [36] B. Cederwall *et al.*, Evidence for a spin-aligned neutron–proton paired phase from the level structure of <sup>92</sup>Pd, *Nature (London)* **469**, 68 (2011).
- [37] M. Honma, T. Otsuka, T. Mizusaki, and M. Hjorth-Jensen, New effective interaction for  $f_5pg_9$ -shell nuclei, *Phys. Rev. C* **80**, 064323 (2009).
- [38] A. Blazhev, M. Gorska, H. Grawe, J. Nyberg, M. Palacz, E. Caurier, O. Dorvaux, A. Gadea, F. Nowacki, C. Andreoiu, G. deAngelis, D. Balabanski, C. Beck, B. Cederwall, D. Curien, J. Doring, J. Ekman, C. Fahlander, K. Lagergren, J. Ljungvall, M. Moszynski, L. O. Norlin, C. Plettner, D. Rudolph, D. Sohler, K. M. Spohr, O. Thelen, M. Weiszflog, M. Wisell, M. Wolinska, and D. Wolski, Observation of a core-excited E4 isomer in <sup>98</sup>Cd, *Phys. Rev. C* **69**, 064304 (2004).
- [39] H. Grawe, K. Straub, T. Faestermann, M. Górska, C. Hinke, R. Krücken, F. Nowacki, M. Bhmer, P. Boutachkov, H. Geissel *et al.*, The ( $6^+$ ) isomer in <sup>102</sup>Sn revisited: Neutron and proton effective charges close to the double shell closure, *Phys. Lett. B* **820**, 136591 (2021).
- [40] F. Ghazi Moradi, B. Cederwall, C. Qi, T. Back, A. Atac, R. Liotta, M. Doncel, A. Johnson, G. deFrance, E. Clement, J. Nyberg, A. Gengelbach, B. M. Nyako, J. Gal, G. Kalinka, J. Molnar, J. Timar, D. Sohler, Z. Dombradi, I. Kuti, K. Juhasz, D. R. Napoli, A. Gottardo, V. Modamio, R. Wadsworth, T. W. Henry, A. J. Nichols, H. Al-Azri, M. Palacz, E. Ideguchi, O. Aktas, A. DiNitto, A. Dijon, T. Huyuk, G. Jaworski, P. R. John, and B. Yilmaz, Spectroscopy of the neutron-deficient  $N = 50$  nucleus <sup>95</sup>Rh, *Phys. Rev. C* **89**, 044310 (2014).
- [41] F. Ghazi Moradi, C. Qi, B. Cederwall, A. Atac, T. Back, R. Liotta, M. Doncel, A. Johnson, G. deFrance, E. Clement, A. Dijon, R. Wadsworth, T. W. Henry, A. J. Nichols, H. Al-Azri, J. Nyberg, A. Gengelbach, T. Huyuk, B.M. Nyako, J. Timar, D. Sohler, Z. Dombradi, I. Kuti, K. Juhasz, M. Palacz, G. Jaworski, S. M. Lenzi, P.R. John, D. R. Napoli, A. Gottardo, V. Modamio, A. DiNitto, B. Yilmaz, O. Aktas, and E. Ideguchi, Character of particle-hole excitations in <sup>94</sup>Ru deduced from  $\gamma$ -ray angular correlation and linear polarization measurements, *Phys. Rev. C* **89**, 014301 (2014).
- [42] T. Fukui, L. De Angelis, Y. Z. Ma, L. Coraggio, A. Gargano, N. Itaco, and F. R. Xu, Realistic shell-model calculations for  $p$ -shell nuclei including contributions of a chiral three-body force, *Phys. Rev. C* **98**, 044305 (2018).
- [43] Y. Z. Ma, L. Coraggio, L. De Angelis, T. Fukui, A. Gargano, N. Itaco, and F. R. Xu, Contribution of chiral three-body forces to the monopole component of the effective shell-model Hamiltonian, *Phys. Rev. C* **100**, 034324 (2019).